

# Design and FDTD Simulation of Photonic Crystal $k$ -Vector Superprism

Takashi MATSUMOTO<sup>†</sup>, Nonmember and Toshihiko BABA<sup>†a)</sup>, Member

**SUMMARY** We theoretically investigated the resolution of the photonic crystal (PC)  $k$ -vector superprism, which utilized the wavelength-dependent refraction of light at an angled output end as a narrow band filter at 1.55  $\mu\text{m}$  wavelength range. Similarly to the case of the conventional  $S$ -vector prism, we defined the equi-incident-angle curve against the dispersion surface, and calculated the beam collimation, wavelength sensitivity and resolution parameters for light propagation in the PC. We estimated that the resolution of the  $k$ -vector prism is the same as or higher than that of the  $S$ -vector prism and the PC can be significantly miniaturized. In addition, we clarified the relation of the  $S$ -vector prism phenomenon and the position of the output end in the  $k$ -vector prism, and different results for the reduced and repeated zone schemes, which are important for the detailed design. We also confirmed that the light propagation simulated by the FDTD method well agreed with the results of the dispersion surface analysis.

**key words:** photonic crystal (PC), superprism, filter, FDTD, WDM

## 1. Introduction

The photonic crystal (PC) is a complex multi-dimensional periodic structure accurately designed by the photonic band theory. It is expected to realize various novel micro-optic devices. Thus far, ultrasmall lasers [1], ultrasmall waveguides [2] and resonant-type narrow band filters [3], all of which utilize the photonic bandgap (PBG), have been reported. On the other hand, an ultralow group velocity and an anomalous dispersion occur at the frequency range higher than the PBG. Especially, the superprism phenomenon has attracted much attention, because it allows wide-angle deflection of light beam by a slight change of the wavelength and the incident angle. It has been theoretically discussed and experimentally demonstrated by Russel [4] and Kosaka, et al. [5]. As applications, a dispersion compensation device [6] and a light deflection device [7] were discussed, but the most fundamental application is a diffraction-type narrow band wavelength filter. In future, a compact, low cost and high performance filter will be desired to realize a wavelength division multiplexing (WDM) network up to end users. But widely used arrayed waveguide grating filter based on silica waveguides is essentially difficult to miniaturize to less than 1  $\text{cm}^2$ . The superprism is expected to solve this problem. However, there were no reports on the quantitative estimation of the wavelength resolution, which is the most important performance of such a filter. Previously, we reported the first theoretical calculation of the

wavelength resolution of the superprism. We used the dispersion surface analysis for the beam collimation parameter  $1/p$ , wavelength sensitivity parameter  $q$ , and the wavelength resolution parameter  $q/p$  in the PC [8]. The result showed that a superprism can realize a sufficiently high resolution usable for the dense WDM, but that the PC cannot still be miniaturized to less than 1  $\text{cm}^2$ .

In this paper, we discuss a novel superprism, which we named the  $k$ -vector superprism. Different from the conventional prism (we named it the  $S$ -vector prism, since it utilizes the deflection of  $S$  vector), the  $k$ -vector prism utilizes the deflection of the  $k$  vector and the refraction of light at an angled output end of a PC. We investigated the resolution of the  $k$ -vector prism using a similar dispersion surface analysis. Figure 1 shows schematics of a square lattice PC and a corresponding dispersion surface. Here, (a) emphasizes the deflection of  $S$  vector, while (b) that of  $k$  vector. In (a), the deflection of  $k$  vector for different wavelengths is smaller than that of  $S$ . In this case, the change of the refraction angle will be small, even if some output end is placed in the PC. Therefore, it is necessary to completely separate the beams inside the PC for the wavelength resolution. This

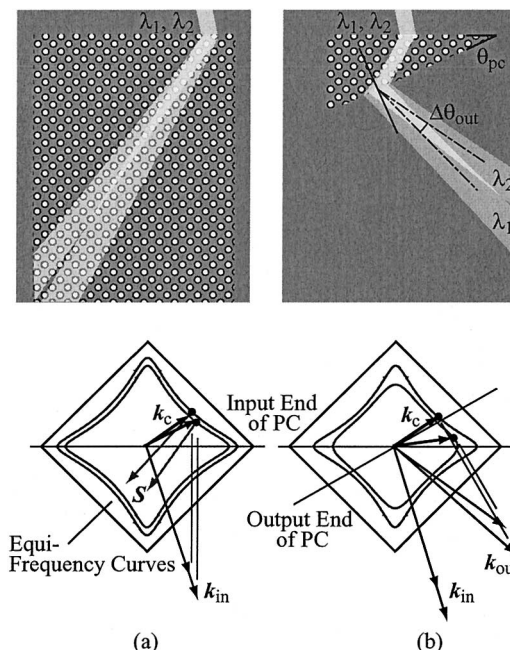


**Fig. 1** Two different types of superprisms in real and  $k$  spaces. 2-D PC is composed of airholes with square lattice rotated by 45°.

Manuscript received October 10, 2003.

Manuscript revised November 27, 2003.

<sup>†</sup>The authors are with Yokohama National University, Yokohama-shi, 240-8501 Japan.

a) E-mail: baba@ynu.ac.jp

is an essential reason that disturbs the miniaturization of the PC in the  $S$ -vector prism. On the other hand, the  $k$  vector is widely changing in (b). At the angled output end of the PC, different  $k$  vectors lead to different refraction angles. This allows the beam separation through the free space propagation outside the PC, so allows the drastic miniaturization of the PC to less than  $(100\ \mu\text{m})^2$ . By integrating a beam focusing lens at the output end or outside of the PC, the length of the free space propagation will be further reduced, so the total filter system will also be miniaturized.

We have already discussed the theoretical calculation of fundamental characteristics of the  $k$ -vector prism in [9]. In this paper, we first present a brief summary of it, and then discuss a relation between the  $S$  vector and the position of the output end, which is important for the design of a  $k$ -vector prism. We also discuss the second Brillouin zone in the repeated zone scheme for the estimation of actual light propagation. Finally, we present the simulation of light propagation against different characteristic parameters by the finite difference time domain (FDTD) method and confirm the correspondence to the dispersion surface analysis.

## 2. Resolution of $S$ -Vector and $k$ -Vector Prisms

We consider a finite width Gaussian beam incident to a two-dimensional PC with a square lattice rotated by  $45^\circ$ , as shown in Fig. 1(a). The deflection angle of the light beam can be analyzed from an equi-frequency curve of a dispersion surface in the Brillouin zone. The wave vector in the PC,  $k_c$ , is determined so that the tangential component of the incident wave vector  $k_{in}$  against the input end of the PC is conserved. The direction of the  $S$  vector is determined by the gradient of the dispersion surface at a point indicated by  $k_c$ . In addition, we consider an equi-incident-angle curve, which is a locus of the point against a constant incident angle and varying frequency of light. Figure 2 shows the disper-

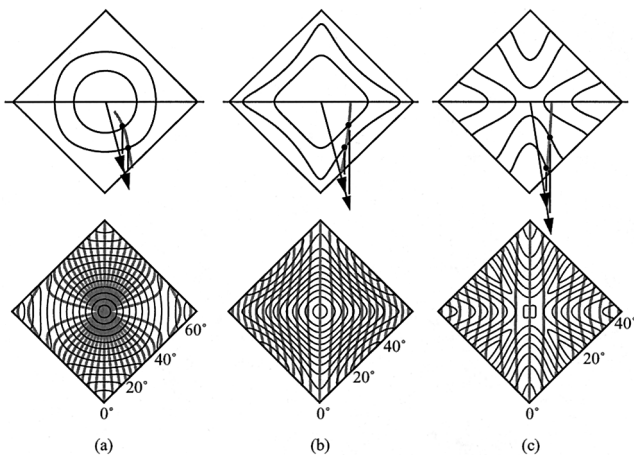


**Fig. 2** Schematics of dispersion surfaces of lower three bands with equi-incident-angle curves (upper) and their calculated examples (lower). (a) First band, (b) second band and (c) third band. Equi-incident-angle curve is drawn with an interval of  $5^\circ$ .

sion surface with equi-incident angle curves for the lowest three photonic bands. For the first band, equi-incident-angle curves shown by gray lines exhibit a radial pattern near the  $\Gamma$  point. For higher bands, which are more important for superprisms, they look like vertical lines. If one aims at a wavelength filter for a certain incident angle, one has to use the dispersion characteristic along the corresponding equi-incident-angle curve.

As shown in Fig. 3, we investigated derivative parameters  $p \equiv (\partial\theta_c/\partial\theta_{in})$ ,  $q \equiv \partial\theta_c/\partial(a/\lambda)$  and  $q/p$  for the  $S$ -vector prism by calculating dispersion surfaces. Here,  $\theta_{in}$  and  $\theta_c$  are beam angles in the incident medium and in the PC, respectively,  $a$  is the lattice constant, and  $\lambda$  is the wavelength. We assumed the background index to be equal to the incident medium index, i.e., 3.065, the index of airholes to be 1.0, and the size of airhole diameter to be  $0.624a$ . The number of plane waves was 37 [8]. In general,  $1/p$  is low and  $q$  is high in  $S$ -vector prisms. This means that the light beam is easily diverged and its propagation is sensitive to the wavelength. The wavelength resolution parameter  $q/p$  exhibits a high value in a limited region along an equi-incident-angle curve. However, this region only allows very narrow latitude of the incident angle; the incident beam must be wide and highly collimated. This is the reason the device size will be of cm order.

We can discuss similar derivative parameters for the  $k$ -vector prism [9]. We calculated the beam collimation parameter  $1/p \equiv (\partial\theta_{out}/\partial\theta_{in})^{-1}$ , the wavelength sensitivity parameter  $q \equiv \partial\theta_{out}/\partial(a/\lambda)$  and the resolution parameter  $q/p$ . Here,  $\theta_{out}$  is the beam angle outside the PC, which is calculated by the conservation law of the tangential component of the  $k$ -vector at the output end. Figure 4 shows  $1/p$ ,  $q$  and  $q/p$  for the second band of the PC with  $45^\circ$  output end. Calculation parameters are the same as for the  $S$ -vector prism. Compared with those of  $S$ -vector prism,  $1/p$  is higher and  $q$  is lower. Note that  $q/p$  exhibits a higher value and much wider latitude of the incident angle. This owes to a wide output beam expanded by the angled output end, which improves the beam collimation outside the PC, and consequently enhances  $q/p$ . At  $\lambda \sim 1.55\ \mu\text{m}$ ,  $q/p \geq 100$  is achieved in a  $\sim 100\ \text{nm}$  wavelength range by an incident beam width of  $13\ \mu\text{m}$ . This almost covers C and L bands of optical fiber communications and allows the butt-joint of

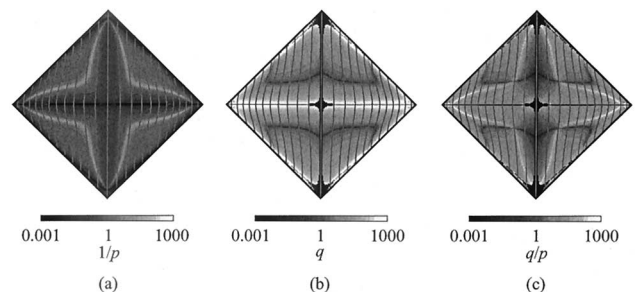


**Fig. 3** Calculated derivative parameters of  $S$ -vector prism. (a) Beam collimation parameter  $1/p$ , (b) wavelength sensitivity parameter  $q$ , and (c) resolution parameter  $q/p$ .

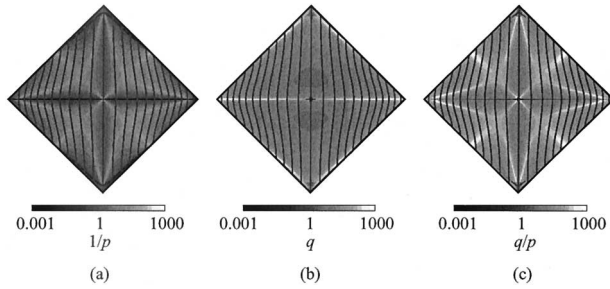


**Fig. 4** Calculated derivative parameters of  $k$ -vector prism with  $45^\circ$  output end. (a)  $1/p$ , (b)  $q$  and (c)  $q/p$ .

a singlemode fiber to the prism. To convert  $q/p$  of the  $k$ -vector prism into an absolute value of the wavelength resolution, the free space propagation has to be calculated with the modeling of the modulated wave front at the output end and an integrated condenser lens. Even without such calculation, we can expect a high resolution for the  $k$ -vector prism, when we consider a fact that the  $S$ -vector prism can achieve a wavelength resolution of 0.4 nm with a resolution parameter of 75.

### 3. Detailed Design and Characteristics

In this section, we first discuss the relation of the beam propagation in the PC and the position of the output end of the  $k$ -vector prism. Although the  $k$ -vector prism utilizes the deflection of the  $k$  vector, the deflection of the  $S$  vector always exists simultaneously. The beam propagation in the PC is determined by the  $S$  vector, so it is necessary to place the output end suitably. Figures 5(a) and (b) show schematics of light propagation in a PC with  $45^\circ$  output end. Light does not necessarily propagate toward the output end, but sometimes toward the other side. For case (b), the output end should be placed at the other side. In the following, we call (a) the front side and (b) the rear side.

Next, we discuss the estimation of light propagation outside the PC using the second Brillouin zone, since the normalized frequency we mainly consider in this study lies in the second Brillouin zone in the extended zone scheme. Figure 6 shows the second dispersion surface in the repeated zone scheme, where both the first and the second Brillouin zones are displayed. The angle of the output end is assumed to be  $45^\circ$ . Directions of light propagation for the front and rear sides are predicted as (a) and (c), respectively, for the first Brillouin zone. Even for the consideration with the second Brillouin zone, we start from  $k_c$  in the first Brillouin zone to discuss the same wave propagating in the PC. Figure 6 describes that  $k_c$  is shifted to the second Brillouin zone by the reciprocal lattice vector.

By adapting the conservation law to the shifted  $k_c$ , direction of light propagation for the front and rear sides are predicted as (b) and (d), respectively. Figure 7 shows  $q/p$  for these four directions, where unusable conditions for each front and rear side are shadowed. The characteristic of  $q/p$  is almost the same between the two sides. The result for

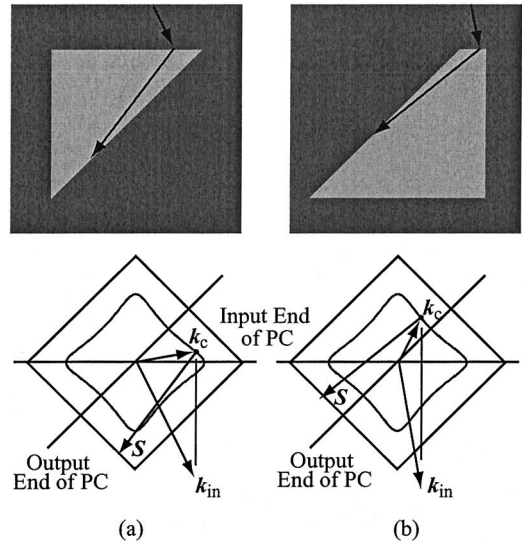


**Fig. 5** Relation of  $S$ -vector prism phenomenon and output end in  $k$ -vector prism. (a) Front side and (b) rear side.

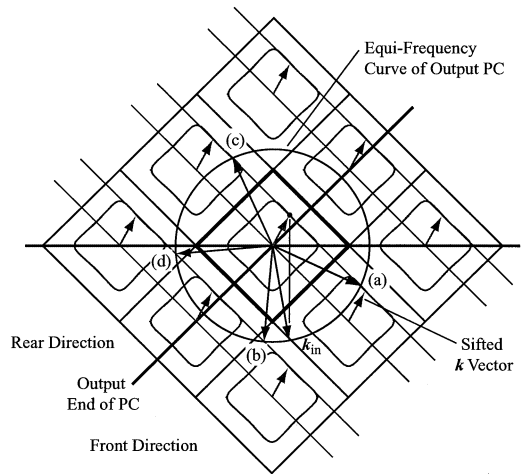


**Fig. 6** Analysis of light propagation by the dispersion surface with the first and the second Brillouin zones. (a) and (b) are results for the front side, and (c) and (d) for the rear side. (a) and (c) are obtained with the first Brillouin zone, and (b) and (d) with the second Brillouin zone.

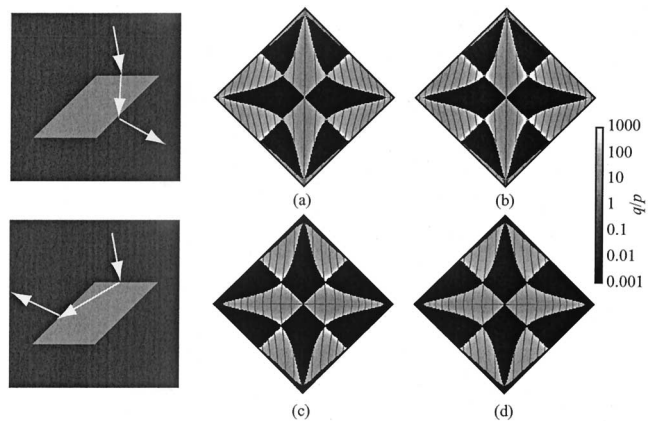


**Fig. 7** Resolution parameter  $q/p$  against the propagation direction of (a)-(d) in Fig. 6. Shaded regions are those which cannot be used as a  $k$ -vector prism.

the second Brillouin zone showed a slightly narrower wavelength range, but almost the same value of  $q/p$ . Thus, the filter performance is equivalent for the four directions. The resolution parameter particularly increases near the boundary of the shadowed region, where the light beam is expanded at the output end so that the collimation parameter is improved.

#### 4. FDTD Analysis

In this analysis, we assumed the same structural parameters as for the analysis in previous sections. The calculation condition is the same as that describe in [7] except that the Yee cell size in this study was  $a/13$ . As an incident wave, a continuous Gaussian beam with a spot diameter of  $250a$  was excited for the magnetic field normal to the 2-D plane,  $H_z$ . This wave was incident to the PC with  $\theta_{in} = 10^\circ$ . Projected airholes were placed at the input end to improve the coupling efficiency [10]. On the other hand, half airholes, which are effective for extracting collimated output beam, were placed at the  $45^\circ$  output end at the rear side. Figure 8 shows an example of field profiles for a high resolution parameter  $q/p = 57$  ( $1/p = 15$  and  $q = 3.8$ ). The dispersion surface analysis predicts that, for a 1.0% frequency change, the output beam is highly collimated with a beam divergence angle of  $\Delta\theta_p < 0.2^\circ$  and a deflection angle  $\Delta\theta_q = 2.2^\circ$ . Drawing lines at  $1/e^2$  of the beam maximum in Fig. 8,  $\Delta\theta_p$  and  $\Delta\theta_q$  were estimated to be  $\Delta\theta_p < 0.2^\circ$  and  $2.3^\circ$ , respectively. Thus, the FDTD calculation well agreed with the dispersion surface analysis. One may think that  $\Delta\theta_q$  is small, but  $\Delta\theta_p$  is so small that the beams can be separated by the free space propagation.

In the previous study, we observed in an FDTD simulation that light output from the PC shows multiple beams, which can be predicted with the first Brillouin zone and many second Brillouin zones [7]. Thus, the direction of output beam is not determined uniquely. In the above re-

sult, however, the optimum condition leads a single output beam, which agrees with Fig. 6(d) for a second Brillouin zone. The result itself is reasonable, when considering the normalized frequency assumed in this simulation. But the reason why the single output beam is obtained is still unclear. It is thought to be due to the airhole shape at the output end and/or due to the condition of refraction. It should be considered in the next study with the detailed consideration of boundary conditions. In addition, as shown in Fig. 8, some amount of reflection is observed at input and output ends. At the final stage of the superprism research, the complete suppression of the reflection by an optimization of the interface structure will be required [10], [11].

#### 5. Conclusion

For the 2-D PC with an angled output end, we discussed the  $k$ -vector superprism instead of the conventional  $S$ -vector prism. From the dispersion surface analysis, we estimated 1) a resolution parameter comparable to or higher than that of the  $S$ -vector prism, 2) over 100 nm usable wavelength range at  $1.55 \mu\text{m}$  wavelength range, and 3) a large latitude of the incident angle, which allows the butt-joint of a singlemode fiber to the prism. Even in the  $k$ -vector prism, the  $S$ -vector prism phenomenon restricts the arrangement of the output end. But it is possible to utilize all conditions by preparing front and rear side output ends. The resolution does not strongly depend on the arrangement of the output end and on the Brillouin zone which is used for the analysis. However, we observed in the FDTD simulation that the beam direction was explained by the analysis with the second Brillouin zone. We also confirmed a highly collimated beam and their angular dispersion.

Thus, the fundamental design theory of the  $k$ -vector prism was almost established. Next issues are to investigate the mechanism that determines the output beam, reduce the reflection loss at interfaces, design a condenser lens for the reduction of free space propagation, and demonstrate a clear filter function in an experiment.

#### Acknowledgements

This work was supported by CREST #530-13 of JST, and by Nano-Photonic and Electron Devices Technology Project of the IT Program, and by 21st COE Program, both from the MEXT.

#### References

- [1] O.J. Painter, A. Husain, A. Scherer, J.D. O'Brien, I. Kim, and P.D. Dapkus, "Room temperature photonic crystal defect lasers at near-infrared wavelength in GaInAsP," *J. Lightwave Technol.*, vol.17, no.11, pp.2082-2088, Nov. 1999.
- [2] T. Baba, N. Fukaya, and J. Yonekura, "Observation of light propagation in photonic crystal optical waveguides with bends," *Electron. Lett.*, vol.35, no.8, pp.654-655, April 1999.
- [3] M. Imada, S. Noda, A. Chutinan, M. Mochizuki, and T. Tanaka, "Channel drop filter using a single defect in a 2-D photonic crystal slab waveguide," *J. Lightwave Technol.*, vol.20, no.5, pp.608-610,

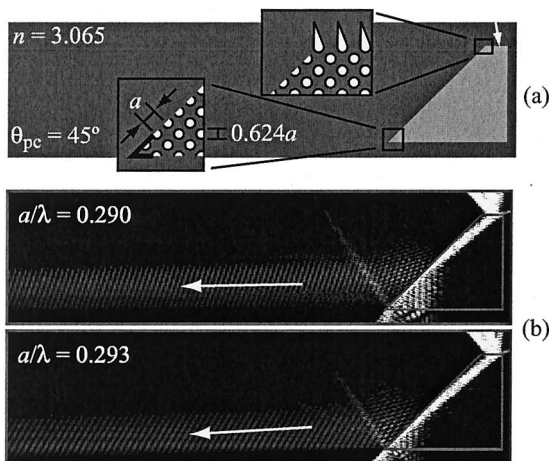


**Fig. 8** Simulated field profiles for a high resolution condition. (a) Calculation model, and (b) profile of  $H_z$  at  $a/\lambda = 0.290$  (upper) and  $0.293$  (lower).

May 2002.

- [4] P.P.St. J. Russell and T.B. Birks, *Photonic Band Gap Materials*, pp.71–91, Kluwer Academic Publishers, Boston, 1996.
- [5] H. Kosaka, T. Kawashima, A. Tomita, M. Notomi, T. Tamamura, T. Sato, and S. Kawakami, “Superprism phenomena in photonic crystals: Toward microscale lightwave circuits,” *J. Lightwave Technol.*, vol.17, no.11, pp.2032–2034, Nov. 1999.
- [6] H. Kosaka, T. Kawashima, A. Tomita, M. Notomi, T. Tamamura, T. Sato, and S. Kawakami, “Photonic crystals for micro lightwave circuits using wavelength-dependent angular beam steering,” *Appl. Phys. Lett.*, vol.74, no.10, pp.1370–1372, March 1999.
- [7] T. Baba and M. Nakamura, “Photonic crystal light deflection devices using the superprism effect,” *IEEE J. Quantum Electron.*, vol.38, no.7, pp.909–914, July 2002.
- [8] T. Baba and T. Matsumoto, “Resolution of photonic crystal superprism,” *Appl. Phys. Lett.*, vol.81, no.13, pp.2325–2327, Sept. 2002.
- [9] T. Matsumoto and T. Baba, “Photonic crystal  $k$ -vector superprism,” *J. Lightwave Technol.*, (2004, to be published)
- [10] T. Baba and D. Ohsaki, “Interfaces of photonic crystals for high efficiency light transmission,” *Jpn. J. Appl. Phys.*, vol.40, no.10, pp.5920–5924, Oct. 2001.
- [11] J. Ushida, M. Tokushima, M. Sirane, and H. Yamada, “Systematic design of antireflection coating for semi-infinite one-dimensional photonic crystal using Bloch wave expansion,” *Appl. Phys. Lett.*, vol.82, no.1, pp.7–9, Jan. 2003.



**Takashi Matsumoto** was born in Shizuoka, Japan, on September 4, 1979. He received the B.E. degree from the Division of Electrical and Computer Engineering, Yokohama National University, Japan, in 2002. Now, he is studying photonic crystal superprism toward the M.E. degree in Yokohama National University.



**Toshihiko Baba** received B.E., M.E. and Ph.D. degrees all from Division of Electrical and Computer Engineering, Yokohama National University (YNU), Japan, in 1985, 1987, and 1990, respectively. During his Ph.D. work, he had been engaged in antiresonant reflecting optical waveguides and lightwave circuits. From 1990, he joined Tokyo Institute of Technology as a research associate. From 1991–1993, he discussed the spontaneous emission control in vertical cavity surface emitting lasers, and achieved the first room temperature continuous wave operation of a long wavelength device. In 1994, he became an associate professor of YNU, and started the research on photonic crystals (PCs) and microdisk lasers (MDLs). Regarding PCs, he reported the first fabrication and characterization of an InP-based light emitters and a line defect waveguide at lightwave frequencies. He also studied a PC light extractor in LEDs. His recent interests are nano lasers and functional devices. Regarding MDLs, he demonstrated the smallest cavity and the lowest threshold, a modified structure named microgear, and near field sensor application. Besides these, he is also active on a deep grating distributed Bragg reflector laser and Si photonic wire waveguides. Dr. Baba is a member of the IEEE/LEOS, JSAP, and American Physics Society. He received the Niwa Memorial Prize in 1991, the Best Paper Award of Micro-Optic Conference in 1993 and 1999, Paper Award and Academic Encouragement Award from IEICE in 1994, and Marubun Research Encouragement Award in 2000.